

Astronomical fibres that solve the problem of the bright infrared sky – first results

J. Bland-Hawthorn,¹ S. Ellis,¹ R. Haynes,² A. Horton,² J.-G. Cuby,^{3,4} T. Birks,⁵ S. Leon-Saval,¹ A. Buryak,¹ V. Steblina,¹ M. Englund,⁶ L. Luo,⁶ G. Edvell,⁶ K. Kolossovski,⁶ M. Puchert,⁶ P. Skovgaard,⁷ D. Noordegraaf,^{7,8} M. Nielsen,⁷ P. Gillingham,² S. Ryder²

A long-standing and profound problem in astronomy is the difficulty in obtaining deep near-infrared observations due to the extreme brightness and variability of the night sky at these wavelengths¹. A solution to this problem is crucial if we are to obtain the deepest possible observations of the early Universe since redshifted starlight from distant galaxies appears at these wavelengths. The atmospheric emission between 1000 nm and 1800 nm arises almost entirely from the de-excitation of OH radicals at ~90 km, giving rise to a forest of extremely bright, very narrow emission lines that varies on timescales of minutes. The astronomical community has long envisaged the prospect of selectively removing these lines, while retaining high throughput between the lines. Such a filter has now been realised and tested for the first time; we present the results of the first on-sky tests. *Our prototype constitutes the most complex optical filter ever constructed. Its use on current 8m and future 30m telescopes will open up many new research avenues in the years to come.*

At visible wavelengths, the terrestrial night sky is very dark which allows astronomers to see back to within a few billion years of the Big Bang using the most powerful optical telescopes on Earth. At infrared wavelengths, the night sky is orders of magnitude brighter due to hydroxyl emission in the upper atmosphere. This is a fundamental obstacle because a great deal of information about the early universe emerges in this part of the spectrum. One approach to bypassing the atmosphere is to launch a space telescope to get above it. This option, however, is hugely expensive and the size of an orbiting telescope is limited.

A solution to the apparently insoluble problem of the infrared night sky emerged in 2004 when our team began to explore new developments in photonics. The infrared sky is bright because the atmosphere glows in hundreds of very narrow spectral lines. Without these lines, the night sky would appear 30-60 times darker. So how do we suppress such a large number of irregularly spaced night-sky lines by factors of hundreds to thousands in an efficient way? Previous attempts using ruled gratings and masks^{1,2} are ultimately flawed because of scattering by the grating and bulk optics³. The hydroxyl emission must be filtered before the light is allowed to enter the spectrograph.

Two technological innovations were required to achieve an efficient sky-suppressing filter. The first was non-periodic fibre Bragg gratings^{4,5} (FBG) capable of suppressing up to 400 narrow lines at high resolution ($\lambda/\delta\lambda \approx 10,000$) and high attenuation (~30dB) over a large bandpass (~200nm) with low attenuation between the lines (<0.2dB). The second innovation was a multi-to-single mode fibre converter,^{6,7} a device we call a “photonic lantern.” Multimode fibres are needed to collect light that has been smeared by atmospheric

turbulence; single mode fibres are required for the gratings. The converters provide efficient interchange between these two formats.

ULTRA BROADBAND FIBRE BRAGG GRATINGS

At the present time, the FBG is the only viable technology to achieving an optical filter with many non-periodically spaced notches^{4,5} and a high degree of suppression (up to 30 dB in transmission) over a very broad spectral band. Further requirements are that each notch must be rectangular and define a narrow wavelength interval ($\delta\lambda=0.16$ nm such that $\lambda/\delta\lambda \approx 10,000$), and the inter-notch transmission must be high (>90%). In astronomical instruments, we propose to form an image by constructing a mosaic of fibres fed by a microlens array⁸.

The principle of the FBG is that light propagating along an optical fibre can be made to reflect at a refractive index modulation printed on the fibre core. If the modulation describes a grating, light can be made to reflect back with high efficiency in a narrow wavelength interval. If the grating period is given by Λ , the reflection efficiency is maximised at the Bragg wavelength $\lambda_B = 2n_{eff}\Lambda$ where n_{eff} (≈ 1.5) is the refractive index of the fibre core before the grating is imposed. The peak reflectivity that can be achieved, $R_g = \tanh^2 \kappa L$, is determined by the grating amplitude κ (in units of cm^{-1}) and the grating length L . The grating amplitude is related to the induced refractive index modulation Δn along the fibre axis z by $\kappa(z) = \pi \Delta n(z) / (2\Lambda(n_{eff} + \langle \Delta n \rangle))$ where z is the distance (in cm) along the FBG. The variable κ is the coupling efficiency of the two counter propagating core modes and defines the grating strength. The quantity $\langle \Delta n \rangle$ is the average refractive index change within the grating modulation.

The maximum amount of information we can impart to the filter design is set by the total length of the FBG and the maximum possible refractive index change $\kappa_{max} = \Delta n_{max} / (2\Lambda n_{eff})$. The total number of data points in the design must be at least $L/\Lambda = 2 \times 10^5$ although the number of optimized parameters is much less. In optimizing the grating design, our goal is to minimise the maximum amplitude of the reflection grating below a practical threshold of $\kappa_{max} \approx 30 \text{ cm}^{-1}$ while keeping the total grating length to 10 cm set by the Mach-Zehnder interferometer.

The coupled-mode system of equations describing light propagation in an FBG is

$$\begin{aligned} \partial E_b / \partial z + i \delta E_b - q(z) E_f &= 0 \\ \partial E_f / \partial z - i \delta E_f - q^*(z) E_b &= 0 \end{aligned} \quad (1)$$

where E_f and E_b are the amplitudes of the forward and backward propagating fields, δ is the frequency normalized to the central Bragg reflection frequency. The function $q(z) = \kappa(z) \exp[i \phi(z)]$, where $\kappa = |q|$ and the phase function $\phi = \text{Arg}(q)$, describes the coupling of forward and backward propagating modes along the FBG. To further complicate the grating design, we require that every notch in the filter profile be as close to rectangular as possible. The target function for the filter shape has the following form:

$$|r_l(k)| = \sqrt{\frac{R_l}{\cosh[2(k - k_l)/\Delta k_l]^4}} \quad (2)$$

where R_l is the peak reflectivity of the l -th channel, k_l is its centre and Δk_l is its width. This choice of reflection profile is typical for FBG designs because it aids convergence even for very complex multi-channel filters. Our multi-channel grating profile can be approximated by

$$q(z) \approx \sum_{l=1}^N G^{-1}[r_l(k)] \quad (3)$$

where $G^{-1}[\cdot]$ is the inverse transform scattering operator and N is the total number of suppression notches. Thus, the coupled equations in (1) present an inverse scattering problem which must be solved iteratively in order to arrive at a practical grating design $q(z)$. How this complex optimization is carried out subject to the above constraints is discussed elsewhere^{4,5}; these references also provides examples of the grating amplitude and phase functions that result from the optimization.

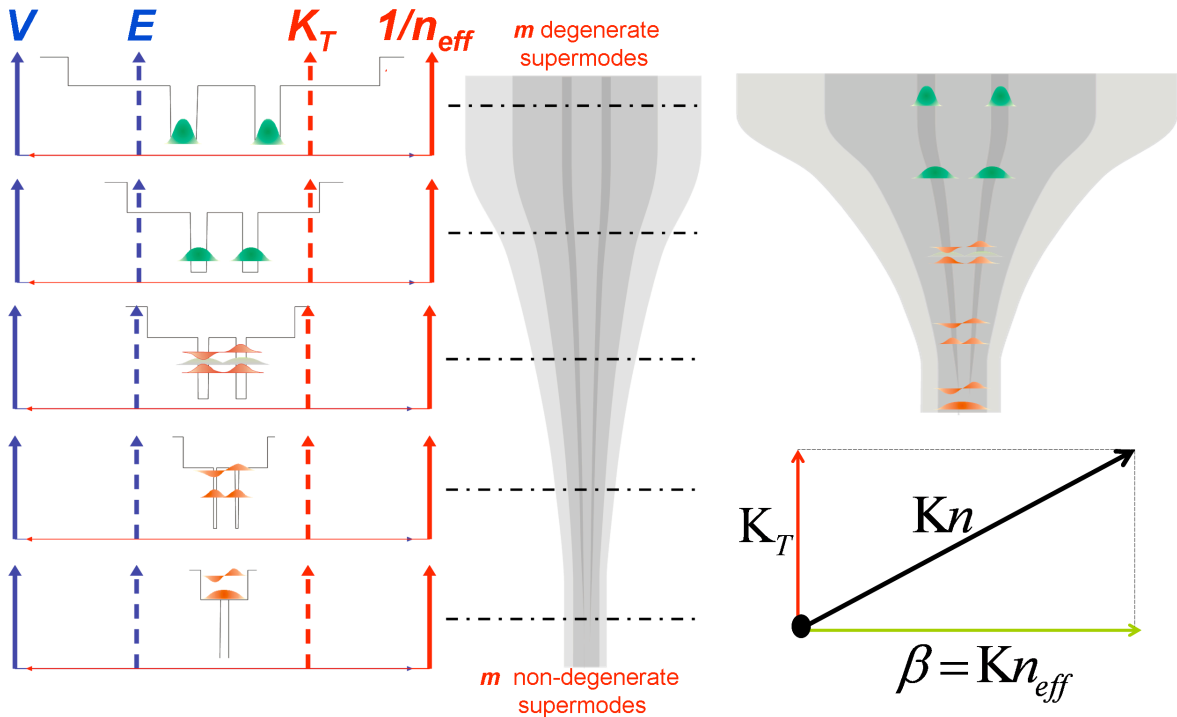


Fig. 1: A photonic lantern consists of two bidirectional tapers that are used back to back (Fig. 2). Here we illustrate the function of one of these tapers starting at the bundle of m SMFs. Initially, the strongly guided radiation in each core is uncoupled; upon entering the adiabatic taper, the radiation is increasingly guided by the cladding. In a perfect system, this leads to m cladding supermodes that evolve to become m spatial electromagnetic modes at the MMF output. A good analogy for the

coupling of radiation between fibre cores is to consider the behaviour of electrons in closely-packed potential wells (see text). The depth of the potential well (V) is equivalent to the reciprocal of the refractive index $1/n_{\text{eff}}$ of the optical waveguide. The energy eigenstate (E) of the electron is equivalent to the transverse component K_T of the wave vector K where the waveguide mode has a propagation constant $\beta = Kn_{\text{eff}}$ (see inset).

PHOTONIC LANTERN

The photonic lantern, first demonstrated⁶ in 2005, features an array of SM fibres surrounded by a low index layer that is adiabatically tapered down to form an MM fibre on input and output (Fig. 2). Efficient coupling is achieved in both directions if the number of (unpolarized) excited modes in the MM fibre is equal to the number of SM fibres in the bundle. At the start of the transition, there are m uncoupled SMFs (Fig. 1). Just how these evolve through an adiabatic taper to become the m electromagnetic spatial modes of the output MMF can be appreciated by analogy with the Kronig-Penney model for the interaction of electrons in a periodic potential well. Initially, each quantum well allows only one electron in its lowest energy state (fundamental mode). The taper transition renders the quantum wells progressively shallower such that each electron begins to tunnel through its barrier. With the wells closer together, the leaky “conduction” electrons behave as if confined to a periodic crystal. At the point where the taper ends, the wells have essentially vanished, and the collective behaviour of the electrons is described by m standing waves (cf. supermodes) confined to a single broad potential well. (Note that the quantum analogy describes the energy eigenstates of an electron, whereas photonics considers the frequency eigenstates of a photon.)

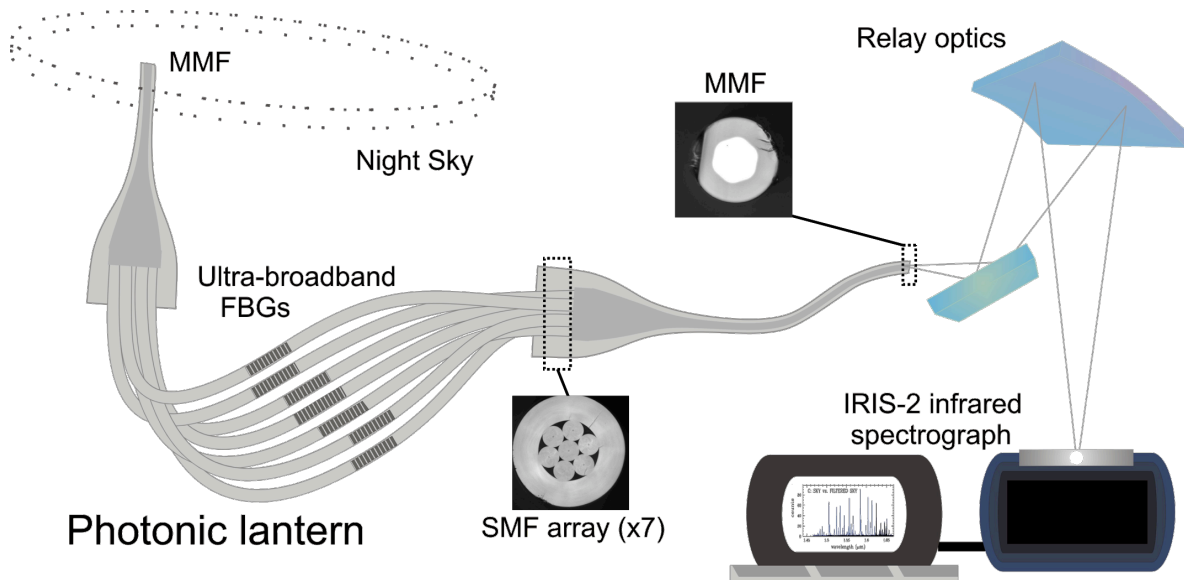


Fig. 2: Schematic showing the set-up for the on-sky tests of the sky-suppressing fibre. The comparison fibre (not shown) has an identical layout except the photonic lantern does not include FBGs. The identical reflection gratings are placed between the two adiabatic tapers.

EXPERIMENT

The sky-suppressing fibres were tested on the nights of 17-19 December 2008 at Siding Spring Observatory in New South Wales, Australia. The end faces of two 60 μ m core fibres were illuminated with light from a $\sim 10^\circ$ patch of sky. Both fibres underwent a taper transition to 7 hexagonally packed single-mode fibres before undergoing another taper transition in reverse back to a multimode fibre (Fig. 2). In one lantern, identical gratings tuned to the 63 brightest OH lines within 1440-1630 nm were printed into the 7 single mode fibres. The other fibre acted as a control, with no gratings. The light from these fibres was relayed into the IRIS-2 infrared spectrograph. Exposures of 900s were taken simultaneously through both fibres, consisting of 31 sequential reads of 30s each in order to minimize detector read noise and to reject charged particle events. The IRIS-2 spectral resolution imposed by the sapphire grism was $\lambda/\delta\lambda \approx 2400$.

In Fig. 3, the results demonstrate the extraordinary power of photonic OH suppression where, for example, no residuals are seen at the locations of the brightest lines. Strong residuals are a feature of essentially all infrared spectroscopic studies in astronomy. The OH lines are suppressed at a resolution four times *higher* than is seen in Fig. 3C. Between the lines, the throughput is high as shown by the OH lines redward of the grating limit. There is a minor insertion loss in our prototype due to imperfect mode matching within the photonic lantern (see Methods). Devices now in development will be capable of converting 61 unpolarized spatial modes to the same number of single-mode tracks allowing for OH suppression within $\sim 100\mu$ m core fibres. Our latest grating designs suppress up to 400 OH lines across the 1000-1800 nm window resulting in a background 30-60 times fainter than is possible today across the entire near infrared window.

The success of our on-sky demonstration shows that the problem of the bright near-infrared night sky has finally been solved. *The prototype constitutes the most complex optical filter ever constructed.* Its application on current 8m telescopes and future 30m telescopes will open up many new research avenues in the coming years.

METHODS

Fibre Bragg Gratings

The refractive index modulation pattern in the FBG comes from exposing the photosensitive fibre core to a spatially varying pattern of UV photons produced by the Mach-Zehnder interferometer. Below 300nm, the UV photons break down the SiO bonds thus causing microscopic variations in the refractive index of the medium. The grating in Fig. 3B is printed onto a GeSiO₂ fibre with a period of $\Lambda = 0.5\mu$ m. The fibre core size of 8.5 μ m allows only single mode propagation. The fibre has a 125 μ m cladding diameter and a 250 μ m acrylate buffer diameter. The required filter is achieved with a low n material ($\approx 10 \text{ cm}^{-1}$) over a long baseline; for our grating, $L \approx 10 \text{ cm}$ and $\langle \Delta n \rangle \sim 10^{-4}$. The wavelength interval for suppression $\Delta\lambda$ is related to the beam psf of the UV laser writing system. The beam psf is given by $z_{\text{psf}} = \lambda_0^2 / (2n_{\text{eff}} \Delta\lambda)$ at an operating wavelength of λ_0 defining the centre of the band. For our first on-sky demonstration, we adopt $\lambda_0 = 1600 \text{ nm}$ and $\Delta\lambda = 200 \text{ nm}$. The derived physical spot size $z_{\text{psf}} = 4 \mu\text{m}$ is a factor of two smaller than what the system

could deliver, requiring us to print the spectral band in two parts, each of length L .

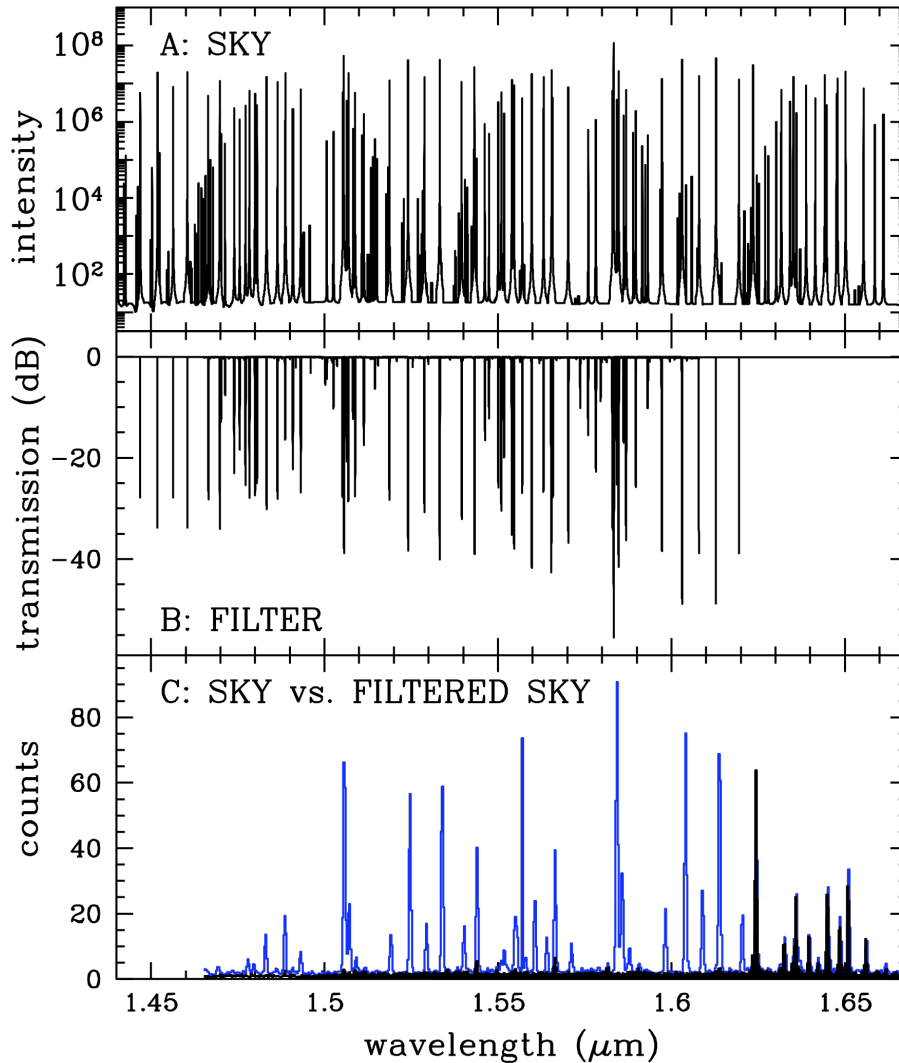


Fig. 3: **A.** Infrared night sky model in units of $\log(\text{phot m}^{-2} \text{s}^{-1} \text{arcsec}^{-2} \mu\text{m}^{-1})$. Faint continuum between the OH lines is from zodiacal scattered light. **B.** Grating transmission in units of dB. The rectangular notch profiles have no detectable ringing and the interline losses are <0.2 dB. **C.** Comparison of the unsuppressed control spectrum (blue) and the suppressed sky spectrum (black). The sky lines are strongly suppressed in the region covered by the gratings. The residual weak continuum is due to starlight in the 10° fibre input beam. The grating region below $1.465\mu\text{m}$ is blocked by the instrument.

Photonic lantern

The lantern is made by inserting 7 SMFs into a glass capillary tube, fusing the bundle together into a solid glass element and tapering the element down to a multimode fibre (MMF) with a core diameter of $\sim 60\mu\text{m}$ and an outer diameter of $\sim 110\mu\text{m}$. The glass tube has a fluor-doped low-index layer on the inside of the capillary wall that acts as the cladding of the down-tapered MMF. The core of the MMF consists of the SMFs fused together. The SMFs are OFS Clearlite fibres, with an

outer diameter of $80\ \mu\text{m}$, a mode field diameter of $7.5\ \mu\text{m}$ and a SM cut-off wavelength below 1500 nm. The tube surrounding the fibres is tapered down by a factor of ~ 3.5 . This results in a V-parameter of the original SMFs in the multimode end of ~ 0.6 at a wavelength of 1550 nm, which means that the light will leak out of the SMFs and be caught by the multimode structure. The tapering of the fibre bundle is done over a length of 4 cm. The tapering of the capillary tube that contains the fibres is done on a GPX-3100 glass processing station from Vytran. By tailoring the amount of heat given to the device during tapering, the point where the fiber bundle is fully collapsed can be controlled. This point is chosen to be (a) where the fibre bundle is fully collapsed; (b) where the V-parameter of the SMFs is reduced by a factor of 2. At a distance of 2-2.5 cm into the taper, the cores are so small that they no longer act as individual waveguides. The diameter of the MMF core is $\sim 60\ \mu\text{m}$ and the NA of the flour ring on the inside of the surrounding tube is 0.06. Therefore, the number of spatial modes that can propagate in the MMF is ~ 13 at wavelengths around 1550 nm. The fabrication method is similar to the “stack-and-draw” technique described in [6].

Acknowledgments

This research has been supported by the Particle Physics and Astronomy Research Council (UK), the Science and Technology Facilities Committee (UK), the Australian Research Council, the Anglo-Australian Observatory, the University of Sydney and the Laboratoire d’Astrophysique Marseille. JBH acknowledges a Federation Fellowship from the Australian Research Council.

Correspondence and request for materials should be addressed to JBH.

Author contributions

JBH has overseen all aspects of the OH suppression project, wrote the manuscript, and performed the experiments with SCE, RH and AJH. TB and SLS were involved in the initial photonic lantern development; the final devices were made by PS, DN and MN. AB and VS were involved in the initial grating development; the final devices were made by ME, LL, GE, KK and MP. JGC, PG and SR were involved in early experiments.

References

1. Maihara, T. *et al.* OH airglow suppressor spectrograph: design and prospects. *Publ. Astron. Soc. Pac.*, **105**, 940 (1993).
2. Ennico, K. *et al.* Cambridge OH suppression instrument (COHSI). *SPIE*, **3354**, 668-674 (1998).
3. Hutley, M.C. *Diffraction Gratings*, Academic Press: New York (1982).
4. Bland-Hawthorn, J., Englund, M.A. & Edvell, G. New approach to OH suppression using an aperiodic fibre Bragg grating. *Optics Express*, **12**, 5902-5909 (2004).
5. Bland-Hawthorn, J., Buryak, A. & Kolossovski, K. Optimization algorithm for ultrabroad multichannel fibre Bragg grating filters. *J. Opt. Soc. Amer. A*, **25**, 153-158 (2008).
6. Leon-Saval, S., Birks, T.A., Bland-Hawthorn, J. & Englund, M.A. Multimode fibre devices with single-mode performance. *Optics Letters*, **19**, 2545-2547 (2005).

7. Noordegraaf, D., Skovgaard, P., Nielsen, M. & Bland-Hawthorn, J. Efficient multi-mode to single-mode coupling in a photonic lantern. *Optics Express*, **17**, 1988-1994 (2009).
8. Parry, I.R. Optical fibres for integral field spectroscopy. *New Astronomy Reviews*, **50**, 301-304 (2006).

¹School of Physics, University of Sydney, Camperdown, NSW 2006, Australia

²Anglo-Australian Observatory, PO Box 296, Epping, NSW 1710, Australia

³Laboratoire d'Astrophysique de Marseille, OAMP, Université Aix-Marseille, France

⁴CNRS, 38 rue Frédéric Joliot Curie, 13388 Marseille cedex 13, France

⁵Department of Physics, University of Bath, Claverton Down, Bath BA2 7AY, UK

⁶Redfern Optical Components, Eveleigh, NSW 1430, Australia

⁷Crystal Fibre A/S, Blokken 84, DK-3460 Birkerød, Denmark

⁸DTU Photonics, Technical University of Denmark, DK-2800, Denmark